The Breakdown Fields and Risetimes of Select Gases Under the Conditions of Fast Charging (~ 20 ns and less) and High Pressures (20 – 100 atmospheres)*

V. Carboni, Titan Pulse Sciences, San Leandro, CA

H. Lackner, Engineering & Technical Services, Oakland, CA

D. Giri, Pro-Tech, Alamo, Ca

J. Lehr, Air Force Research Laboratory, Kirtland AFB

Introduction

An interest in wide-band impulse radar systems has brought about the need to develop phased antenna arrays that can focus and steer an electromagnetic pulse in the far field. To produce useful radiated signal levels in the far-field, these arrays will need to be driven by high voltage, high power sources that at least in the short term may rely on pulsers using gas spark gap technology. To produce the high frequencies necessary, an array must be driven by sources with a risetime in the range of 100-200 pico-seconds or even faster. Since multiple pulsers will have to be used to drive a large array, a suitable pulser design will most importantly have to have ultra-low triggering jitter (the standard deviation in the switch closure delay after trigger arrival). The jitter will have to be some relatively small fraction of this risetime to accurately synchronize the array to steer and preserve the risetime. This implies a jitter ideally in the 10's of pico-second range. Although risetimes can routinely be achieved in the desired range, the jitter requirement represents a breakthrough in spark gap technology.

A preliminary gas characterization investigation preceded the development of such a fast risetime, ultra-low jitter triggered spark gap based pulser. This paper describes the results of this investigation that looked at the breakdown fields and risetimes for a variety of commonly used gases in the field of pulse power. The gases studied included SF6, air, 15 and 30% SF6/Air mixes, nitrogen, and hydrogen.

The goals of this investigation were to:

- Characterize the breakdown field vs. pressure and examine the effects of:
    - Polarity
    - Varying stress times
    - Uniform field vs. point-plane
- Compare the actual measured resistive phase risetimes to calculations

**Work supported by SBIR Phase II Contract No. F29601-99-C-0165.*

Test Fixture

A 16.5-ohm monocone design was chosen to evaluate the gases. The reason for using a monocone was to provide a well-defined geometry of calculable and constant impedance that was unobstructed for a sufficient clear time in order to be able to measure the arc risetime and compare it to calculation. The monocone is shown in schematic form in Figure 1.

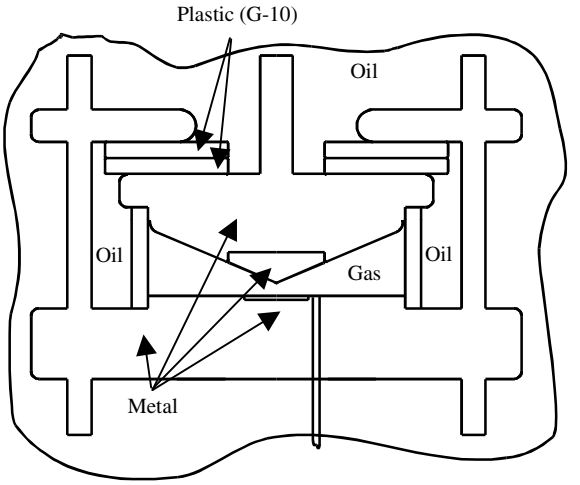

Figure 1. Monocone test fixture.

The cone was designed to be safely pressurized to 100 atmospheres with any of the candidate gases including hydrogen. The inner diameter of the pressurized vessel envelope was approximately 8 inches and approximately 3 inches long. The conical shaped plate within the vessel was the charged end and the opposing flat plate was the monocone's ground plane.

The conical charged plate was sandwiched between the ground plane and a second steel annular plate that was also grounded. The charged cone was insulated from this second plate by two stacked layers of ½-inch thick G-10 plastic. A stalk connected to the cone extended through the hole in the annular plate and was connected to the charging input lead from the Marx. The two grounded steel plates were bolted together with 12 steel tie rods that

0-7803-7120-8/02/$17.00 © 2002 IEEE

Report Documentation Page

Form Approved
OMB No. 0704-0188

1. REPORT DATE	2. REPORT TYPE	3. DATES COVERED
JUN 2001	**N/A**	**-**

4. TITLE AND SUBTITLE	5a. CONTRACT NUMBER
The Breakdown Fields and Risetimes of Select Gases Under the Conditions of Fast Charging (~ 20 ns and less) and High Pressures (20 100 atmospheres)*	5b. GRANT NUMBER
	5c. PROGRAM ELEMENT NUMBER
6. AUTHOR(S)	5d. PROJECT NUMBER
	5e. TASK NUMBER
	5f. WORK UNIT NUMBER
7. PERFORMING ORGANIZATION NAME(S) AND ADDRESS(ES) **Titan Pulse Sciences, San Leandro, CA**	8. PERFORMING ORGANIZATION REPORT NUMBER
9. SPONSORING/MONITORING AGENCY NAME(S) AND ADDRESS(ES)	10. SPONSOR/MONITOR'S ACRONYM(S)
	11. SPONSOR/MONITOR'S REPORT NUMBER(S)

12. DISTRIBUTION/AVAILABILITY STATEMENT

Approved for public release, distribution unlimited

13. SUPPLEMENTARY NOTES

See also ADM002371. 2013 IEEE Pulsed Power Conference, Digest of Technical Papers 1976-2013, and Abstracts of the 2013 IEEE International Conference on Plasma Science. IEEE International Pulsed Power Conference (19th). Held in San Francisco, CA on 16-21 June 2013. U.S. Government or Federal Purpose Rights License.

14. ABSTRACT

An interest in wide-band impulse radar systems has brought about the need to develop phased antenna arrays that can focus and steer an electromagnetic pulse in the far field. To produce useful radiated signal levels in the farfield, these arrays will need to be driven by high voltage, high power sources that at least in the short term may rely on pulsers using gas spark gap technology. To produce the high frequencies necessary, an array must be driven by sources with a risetime in the range of 100-200 picoseconds or even faster. Since multiple pulsers will have to be used to drive a large array, a suitable pulser design will most importantly have to have ultra-low triggering jitter (the standard deviation in the switch closure delay after trigger arrival). The jitter will have to be some relatively small fraction of this risetime to accurately synchronize the array to steer and preserve the risetime. This implies a jitter ideally in the 10s of pico-second range. Although risetimes can routinely be achieved in the desired range, the jitter requirement represents a breakthrough in spark gap technology.

15. SUBJECT TERMS

16. SECURITY CLASSIFICATION OF:			17. LIMITATION OF ABSTRACT	18. NUMBER OF PAGES	19a. NAME OF RESPONSIBLE PERSON
a. REPORT	b. ABSTRACT	c. THIS PAGE			
unclassified	**unclassified**	**unclassified**	**SAR**	**5**	

transferred the compressive forces to the cone through the annular G-10 sheets.

The electrodes of the gap were stainless steel and the gap of the monocone configuration was 0.091 cm that had an enhancement of about 1.38. For point-plane breakdown testing, the monocone apex tip was replaced with a needle-like shank of approximately 0.046-cm diameter with a gap of 0.18 cm.

The monocones ground plane was equipped with several D-dot ports. Two were positioned 3 cm from the apex and another positioned 6.4 cm from the apex. The clear-time of the wavefront is determined by the two-way transit time between the position of the D-dot and the impedance discontinuity of the vessel wall. The clear-times were approximately 560 pico-seconds for the closest D-dots and about 250 pico-seconds for the furthest D-dot from the apex.

The estimated D-dot risetime is 25 pico-seconds which is approximately determined by the transit time of a wave across the end of the 0.25 inch diameter semi-rigid cable cut off flush with the ground plane. The D-dot was calibrated against a liquid resistive monitor that was itself calibrated against a reference monitor using standard traceable techniques. The D-dot was used to measure risetime while the resistive monitor measured the voltage amplitude.

A TDS 684C with a bandwidth of 1 GHz was used to record the charging waveforms for determining the charge time and amplitude. An SCD 5000 with a bandwidth of 4.5 GHz was used to measure the output risetime. The cable from the monocone to the SCD-5000 oscilloscope was ½-inch diameter Foamflex used in conjunction with a DC-11 compensated delay line. The throughput risetime of the SCD 5000, cabling, and delay line was estimated to be 100 pico-seconds.

Circuit

The monocone test fixture was driven by a six-stage gas insulated Marx capable of achieving an output voltage into an open circuit of 600 kV. The circuit schematic is shown in Figure 2 where the erected capacitance of the Marx (CM) was 425 pF. The monocone load (Cmono) was represented by a capacitance of 210 pF whose value was brought about by the relatively high dielectric, sandwiched G-10 plastic sheet construction. An additional 300 ohms (RS) was placed between the Marx and the monocone to limit the late-time current through the arc channel. This minimized the wear on the electrode tips and possible degradation of the measured breakdown fields.

An important parameter that was varied was the application time of the voltage on the gap, which defined the effective stress time. The effective stress time, referred to as t_{eff}, is defined as the time the voltage exceeds a level of 89% of its peak prior to breakdown.

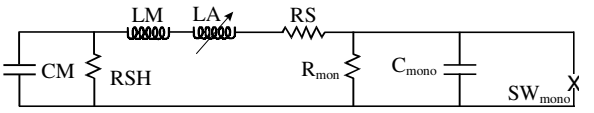

Figure 2. Gas breakdown monocone circuit.

The value of t_{eff} is measured from each charging waveform as the time between the 89% level and the 100% level, which is where the gap broke down. The stress time was varied by either of two means. One method was to place an additional 16 µH (LA) in series with the Marx that increased the charge time by a factor of about four times. Another was to vary the dc charge voltage of the Marx and consequently the Marx output voltage for a given pressure. By going to a higher Marx output voltage the breakdown voltage level was achieved in a shorter time. The range of stress times achieved using these methods in combination was approximately 1 to 5 nanoseconds

Near Uniform-Field Breakdown vs. Pressure

The near-uniform monocone peak breakdown fields for negative polarity on the cone tip are plotted against pressure in Figure 3. The stress times for this group of data varied from approximately1 to 5 ns. The maximum pressures of SF6 and its mixes were limited because of the onset of liquefication at higher pressures.

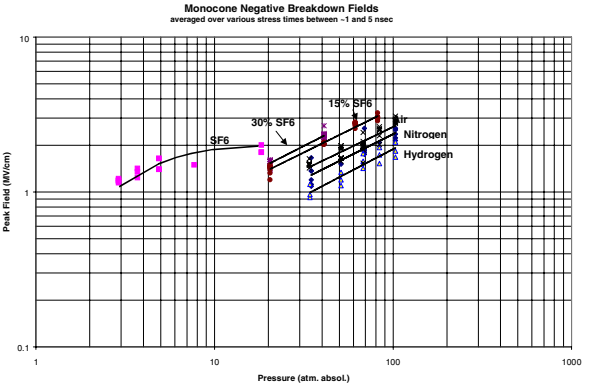

Figure 3. Monocone negative breakdown fields.

It was a little surprising that the breakdown of air exceeded nitrogen by about 10%. Normally for lower pressures and longer charge times nitrogen breakdown would be expected to exceed that of air by about 10%. It is possible that this is related to the higher pressure and faster time regime. Similar results were observed for positive polarity on the cone tip where the breakdown fields were about 10% lower than the negative. Table 1 compares the fields for the two polarities at select pressures.

The breakdown field scaling with pressure usually follows a $p^{0.7}$ relationship for lower pressures and longer stress times. The results of the experiment are summarized in Table 2. They show a slightly weaker relationship that possibly is brought about by a tendency of the breakdown fields to flatten at the much higher pressures tested.

Table 1. Summary of breakdown feild strengths for the mildly-enhanced monocone gap.

Gas	Pressure (atm. abs.)	Polarity	Peak Breakdown Field (MV/cm)	Mean Breakdown Field (MV/cm)
SF6	18.3	Neg	1.86	1.35
Air	85	Neg	2.40	1.74
Air	85	Pos	2.15	1.56
N2	85	Neg	2.10	1.52
N2	85	Pos	2.10	1.52
H2	85	Neg	1.70	1.23
H2	85	Pos	1.65	1.20
15% SF6/ 85% Air	85	Neg	3.05	2.21
15% SF6/ 85% Air	85	Pos	3.10	2.25
30% SF6/ 70% Air	41	Neg	2.25	1.63
30% SF6/ 70% Air	41	Pos	2.o5	1.49

Table 2. Pressure dependency of monocone breakdown field.

Gas Type	Negative Polarity Pressure Scaling Exponent n Where $F=Kp^n$	Positive Polarity Pressure Scaling Exponent n Where $F=Kp^n$
Air	0.56	0.47
Nitrogen	0.66	0.60
Hydrogen	0.60	0.40
15% SF6/85% Air	0.57	0.62
30% SF6/70% Air	0.59	0.51

Breakdown Field vs. Stress Time

The breakdown field dependency on the applied voltage stress time tended to be strongest at the lower pressures near 30 atmospheres and diminish or in some cases disappear as the pressure was raised towards 100 atmospheres. A typical example of this tendency is that shown in Figure 4 where the positive polarity hydrogen gas breakdown is plotted. Included in the plot is a data point later gotten in the subsequent pulser tests for a stress time of only 0.3 ns and a pressure of 100 atm. It seems to fall on the extrapolated trend line for ~100 atm. pressure confirming the trend for this pressure.

Obviously, the breakdown fields for the low pressures would not be expected to converge to the same value as for the high pressures as suggested in Figure 4. Thus, it is likely that the low pressure breakdown fields would actually level off as the stress times decreased due to other breakdown mechanisms coming into play or that their slopes would be found to be less steep if fitted to a wider range of stress times.

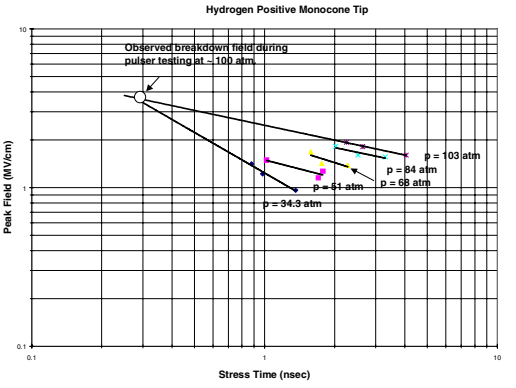

Figure 4. Hydrogen positive monocone tip.

This observed stress time dependency could possibly be explained in terms of the formative times of the gap and its variation with pressure and field strength. The formative time of a gap is the time that streamer growth develops just prior to the gap closing. After the voltage is applied, there is a delay during which free electrons appear. Once the free electrons are made available, the avalanching processes begin. The time duration during which the avalanching process occurs is the formative time. Pulsed breakdown exceeds the static breakdown of the gap because of this time lapse.

During subsequent pulser tests, the formative time for the high end of the pressure range of the tested gases were measured and found to be approximately 1-2 ns; much shorter than the charge times used in these gas tests. Although not specifically measured during this experiment, the literature cites examples of formative times for long charge times and low pressures in the range of 10's of nsec or more; longer than the charge times used in these gas tests.

When the formative time is much shorter than the range of charge times as it is at the high pressure, little over-voltage occurs during this formative time lapse even as the charge time is decreased within this range. This results in little or no dependence of breakdown field on pressure as observed. Just the opposite effect occurs when the formative time is longer than the charge time as it was at the lower pressures.

Point-Plane Breakdown Field vs. Pressure and Stress Time

For the point-plane gap using nitrogen, hydrogen or either of the two SF6 mixes, the breakdown fields across the tested pressure range were generally weaker when the highly enhanced electrode was positive polarity as illustrated in Figure 5 showing the results for nitrogen and hydrogen. The exception was hydrogen where the breakdown fields at the lowest pressure of about 14 atmospheres were similar for both polarities. The differences in the breakdown fields for the two polarities are more apparent when the pressure is increased.

For both nitrogen and hydrogen (Fig. 5), the positively enhanced breakdown seems to peak out and flatten at about 80 atmospheres. For the 15% air/SF6 mix as shown in Figure 6, the opposite was observed where the negatively enhanced breakdown fields seem to peak out and flatten or roll over at 80 atmospheres. Insufficient data exists to draw any conclusion regarding behavior of the 30% air/SF6 mix.

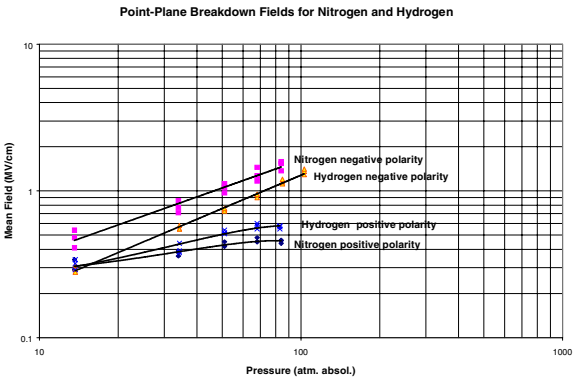

Figure 5. Point-plane breakdown fields for N2 and H2.

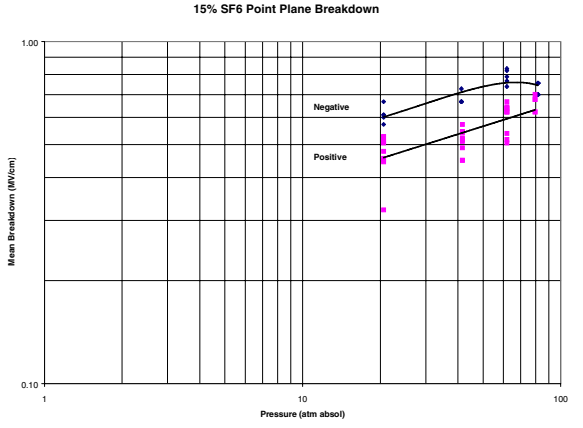

Figure 6. 15% SF6 point-plane breakdown.

Table 3 compares the point-plane mean breakdown fields with those of the monocone mean fields for nitrogen, hydrogen, and the two air/SF6 mixes at select pressures. Columns 3 and 4 list the mean breakdown fields for both enhanced negative and positive polarities and column 5 compares the two. Column 6 compares the mean mono-cone fields with the mean point-plane fields.

Risetime Measurements

Risetime data with the monocone geometry was obtained for hydrogen, nitrogen and the two SF6 mixes at both the low and high ends of the pressures tested and for both positive and negative polarities. The data is presented in Table 4.

The table shows the breakdown field with the 10-90% measured and diagnostic and instrumentation bandwidth corrected risetimes. The inductive risetime of the gap was estimated at 160 psec based on ~15 nH per cm of arc channel length. The inputted resistive phase risetime was calculated by quadrature subtraction of this inductive risetime from the corrected measured risetime. These resistive phase risetimes are compared to the calculated risetimes in column 9 which are derived from the JC Martin formula:

$$\tau_{resistive}(10-90\%)=\left(158\sqrt{\rho/\rho\,(air)}\Big/\left((F)^{4/3}\,(Z)^{1/3}\right)\right)ns$$

where

ρ = density of the gas
ρ = density of air at STP
F = breakdown field in 10kV/cm units
Z = driven impedance in ohms.

Table 3. Summary of enhanced breakdown field strengths.

Gas	Press. (atm. abs)	Neg. Mean Breakdown Field (MV/cm)	Pos. Mean Breakdown Field (MV/cm)	Mean E(Pos)/ E(Neg)	Mean E(PP)/ E(uniform)
SF6	14.3	0.92	--	--	0.71(neg)
N2	14.3	0.46	0.31	0.67	0.85(neg) 0.30 (pos)
N2	85	1.4	0.47	0.34	0.85(neg) 0.30(pos)
H2	14.3	0.29	0.31	~1	
H2	85	1.25	0.59	0.47	~1(neg) 0.5 (pos)
15% SF6 / 85% Air	21	0.60	0.45	0.75	
15% SF6 / 85% Air	80	0.78	0.49	0.79	0.35(neg) 0.28(pos)
30% SF6 / 70% Air	21	0.68	0.49	0.72	
30% SF6 / 70% Air	41	0.76	0.60	0.79	0.47(neg) 0.40(pos)

The results show that in all cases the risetime is fastest when the monocone tip is negative rather than positive suggesting that a negatively initiated streamer has a faster risetime. For the most part, the formula is overly pessimistic in predicting the risetime. Better predictions are obtained at the higher pressures. The formula does however predict the right ordering of the risetimes of the gases.

Conclusions

The breakdown fields measured within the ranges of approximately 20 to 100 atmospheres and within the stress times of 1 to 5 ns seemed to be roughly consistent with what is observed at lower pressures and longer stress times. The dependency of the breakdown field on pressure was slightly weaker than the $p^{0.7}$ generally observed.

The dependency of the breakdown fields on pressure and stress time is thought to be due to formative time issues. The time dependency went away when the formative time was very much less that the pulse application time which occurred at the highest pressures tested.

Hydrogen exhibits a polarity effect for point plane breakdown. At low pressure this effect disappears but is most apparent at high pressure. Both hydrogen and nitrogen positive polarity point plane fields begin to roll off at high pressure unlike the negative polarity which continues to increase with pressure. The 15% SF6 mix exhibits a rolling off of the field in the negative polarity. In all cases the enhanced negative polarity is stronger than positive polarity.

The resistive phase risetime formula seems to be overly pessimistic in predicting risetimes but it gives the right ordering of the risetime with the gas type. The formula is generally more accurate at the higher pressures.

Table 4. Monocone risetime data summary.

Gas	Polarity	Pressure (Abs. atm.)	Breakdown Field (MV/cm)	Measured Risetime (psec)	Corrected Risetime[1] (psec)	Est. Inductive Risetime[2] (psec)	Inputted Resistive Phase Risetime[3] (nsec)	Calcu. Resistive Phase Risetime (nsec)
N2	N	85	2.25	300	282	160	232	430
N2	P	85	2.20	324	308	160	269	430
N2	N	34.3	1.20	292	274	160	222	594
N2	P	34.3	1.28	325	309	160	264	594
H2	N	85	1.82	207	181	160	84	155
H2	P	85	1.78	231	208	160	132	155
H2	N	34.3	0.91	200	173	160	66	253
H2	P	34.3	0.90	240	218	160	148	253
15% SF6	N	82.4	3.02	259	239	160	178	204
15% SF6	P	82.4	3.07	272	253	160	196	204
15% SF6	N	21	1.36	255	235	160	172	297
15% SF6	P	21	1.3	274	255	160	199	297
30% SF6	N	41	2.35	247	226	160	160	231
30% SF6	P	41	2.02	290	272	160	220	285
30% SF6	N	21	1.52	267	248	160	189	298
30% SF6	P	21	1.38	285	267	160	214	339

1 assumes measurement system risetime ~100 psec

2 assumes inductance ~15 nH/cm

3 $\tau(\text{measured})^2 - \tau(\text{inductive})^2 = \tau(\text{resistive})^2$